

RSC Advances



This is an *Accepted Manuscript*, which has been through the Royal Society of Chemistry peer review process and has been accepted for publication.

Accepted Manuscripts are published online shortly after acceptance, before technical editing, formatting and proof reading. Using this free service, authors can make their results available to the community, in citable form, before we publish the edited article. This *Accepted Manuscript* will be replaced by the edited, formatted and paginated article as soon as this is available.

You can find more information about *Accepted Manuscripts* in the [Information for Authors](#).

Please note that technical editing may introduce minor changes to the text and/or graphics, which may alter content. The journal's standard [Terms & Conditions](#) and the [Ethical guidelines](#) still apply. In no event shall the Royal Society of Chemistry be held responsible for any errors or omissions in this *Accepted Manuscript* or any consequences arising from the use of any information it contains.

Cite this: DOI: 10.1039/c0xx00000x

www.rsc.org/ RSC Advances

PAPER

Hybrid Ternary Composites of Hyperbranched and Linear Polyimides with SiO₂: A Research for Low Dielectric Constant and Optimized Properties

Seongku Kim¹, Xingyuan Wang¹, Shinji Ando^{2*}, and Xiaogong Wang^{1*}

⁵ Received (in XXX, XXX) Xth XXXXXXXXXX 20XX, Accepted Xth XXXXXXXXXX 20XX
DOI: 10.1039/b000000x

Based on a hydroxyl-terminated hyperbranched polyimide (HBPI_{BPADA-TAP(OH)}), two series of hybrid ternary composites composed of a linear polyimide (PI_{6FDA-APB}), HBPI_{BPADA-TAP(OH)} (10% and 20%), and various concentrations of SiO₂ were fabricated by sol-gel method. Research showed that properties of the composites are closely related with the ratio of HBPI_{BPADA-TAP(OH)} to SiO₂, which can be optimized by proper choice of the compositions. Under the optimized conditions, the hybrid ternary composites show properties complementary at the drawbacks of unary or binary systems. The dielectric constant (D_k) of the PI_{6FDA-APB}-HBPI_{BPADA-TAP(OH)}-10%-SiO₂-10% composite reaches the lowest value of 2.26. The silica loading and reinforcement binding with PI_{6FDA-APB}-HBPI_{BPADA-TAP(OH)} matrix are confirmed by the SEM morphology of the hybrid ternary composite films. When a suitable amount (20%) of HBPI_{BPADA-TAP(OH)} is added into the PI_{6FDA-APB}-SiO₂-10% composite, the optical transmittance is significantly improved to be 63% at the wavelength of 450 nm. With increasing the content of SiO₂, the thermal expansion is obviously reduced. For the PI_{6FDA-APB}-HBPI_{BPADA-TAP(OH)}-10%-SiO₂-30% composite, the coefficient of thermal expansion (CTE) of the film is reduced to 15.9 ppm °C⁻¹ compared to 37.1 ppm °C⁻¹ for the PI_{6FDA-APB} film (reducing about 59%). Due to these optimized properties, hybrid ternary composite films are expected to have potential applications in micro-electronic insulator fields such as interlayer dielectric of advanced electronic devices.

RSC Advances Accepted Manuscript

* 1. Department of Chemical Engineering, Laboratory of Advanced Materials (MOE), Tsinghua University, Beijing, 100084, P. R. China Corresponding

author: email wxc-dce@mail.tsinghua.edu.cn

* 2. Department of Chemistry & Materials Science, Tokyo Institute of Technology, Ookayama 2-12-1-E4-5, Meguro-ku, Tokyo, 152-8552, Japan
email sando@polymer.titech.ac.jp

Cite this: DOI: 10.1039/c0xx00000x

www.rsc.org/ RSC Advances

PAPER

Introduction

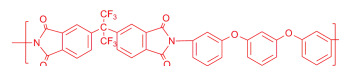
Polyimide (PI) has been widely studied during the past decades and the development of the low dielectric constant PI for electronic industry has been a focus of recent investigations.¹⁻⁵

The insulating interlayer materials with low dielectric constant are urgently needed in order to improve the speed or reduce resistance capacitance (RC) delay time of electron flow transmission between the chips of large scale integrated circuit and meet the requirement of high integration.¹ In recent years, different approaches have been explored to develop PIs with ultra-low dielectric constants, which include well-designed organic-inorganic systems,^{2, 6, 8} systems with air gap or pore voids,^{7, 8} low polarization,⁹⁻¹¹ and increased free volume.^{6, 7, 9, 10, 12} However, for unary or binary systems, there are some limitations for their applications as insulating materials, such as the low thermal mechanical or low transparency properties.^{6, 7, 9, 10, 12} Ideal insulating materials should not only possess low dielectric properties, but also show high transparency and excellent thermal mechanical properties. In order to improve these properties, hybrid ternary composites composed of a hydroxyl-terminated hyperbranched polyimide, a linear polyimide and inorganic silica can be a new approach to significantly improve the properties.¹³

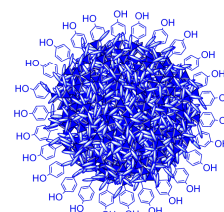
Hyperbranched polymers (HBPs) are well known for their unique properties, such as possessing a large number of end groups, low solution viscosity, high solubility and others.¹⁴⁻¹⁷ It can be used to show improved properties when compared with their linear analogues. In recent years, hyperbranched polyimide (HBPI) has been synthesized,¹⁸ characterized,¹⁹ and used for applications such as gas permeability.^{20, 26} Those studies showed that there were many open and accessible cavities (typically several angstroms in size) in a rigid branched structure.^{6, 21, 22} Those unique characteristics can be used for the development of low dielectric constant polyimide.^{23, 24} Our previous study has showed that by using a hyperbranched polyimide (HBPI)_{BPADA-TAP(OH)} as the third component, dielectric and other properties can be significantly improved for the hybrid ternary systems.¹³ The research also showed that the HBPI_{BPADA-TAP(OH)} and SiO₂ are two key components in the ternary composites to improve the properties. However, the proper ratios and compositions of the components to optimize the properties are still not understood and require further investigations.

In this study, we prepared and investigated the hybrid ternary composites composed of HBPI_{BPADA-TAP(OH)}, a linear polyimide (PI_{6FDA-APB}) and inorganic silica (Scheme 1) with different compositions. HBPI_{BPADA-TAP(OH)} was synthesized via the A₂ + B₃ polycondensation²⁶ and peripheral-group modification after polymerization.¹³ The hybrid ternary composite films were fabricated by a sol-gel process. We studied the hybrid ternary composites by FTIR, UV-Vis, SEM, thermal analysis, dielectric and mechanical analyzers to find the ways to reduce dielectric constant and improve other properties. The properties and their relationships with compositions of the hybrid ternary composites

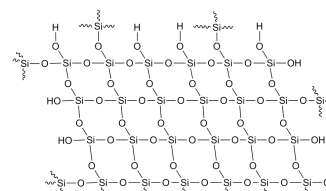
were investigated. The composites with optimized compositions have the complementary effects to improve the weakness of the unary or binary system. The results are reported in the following sections in detail.



Linear PI Backbone



Hydroxy terminated Hyperbranched polyimide (HBPI(OH))



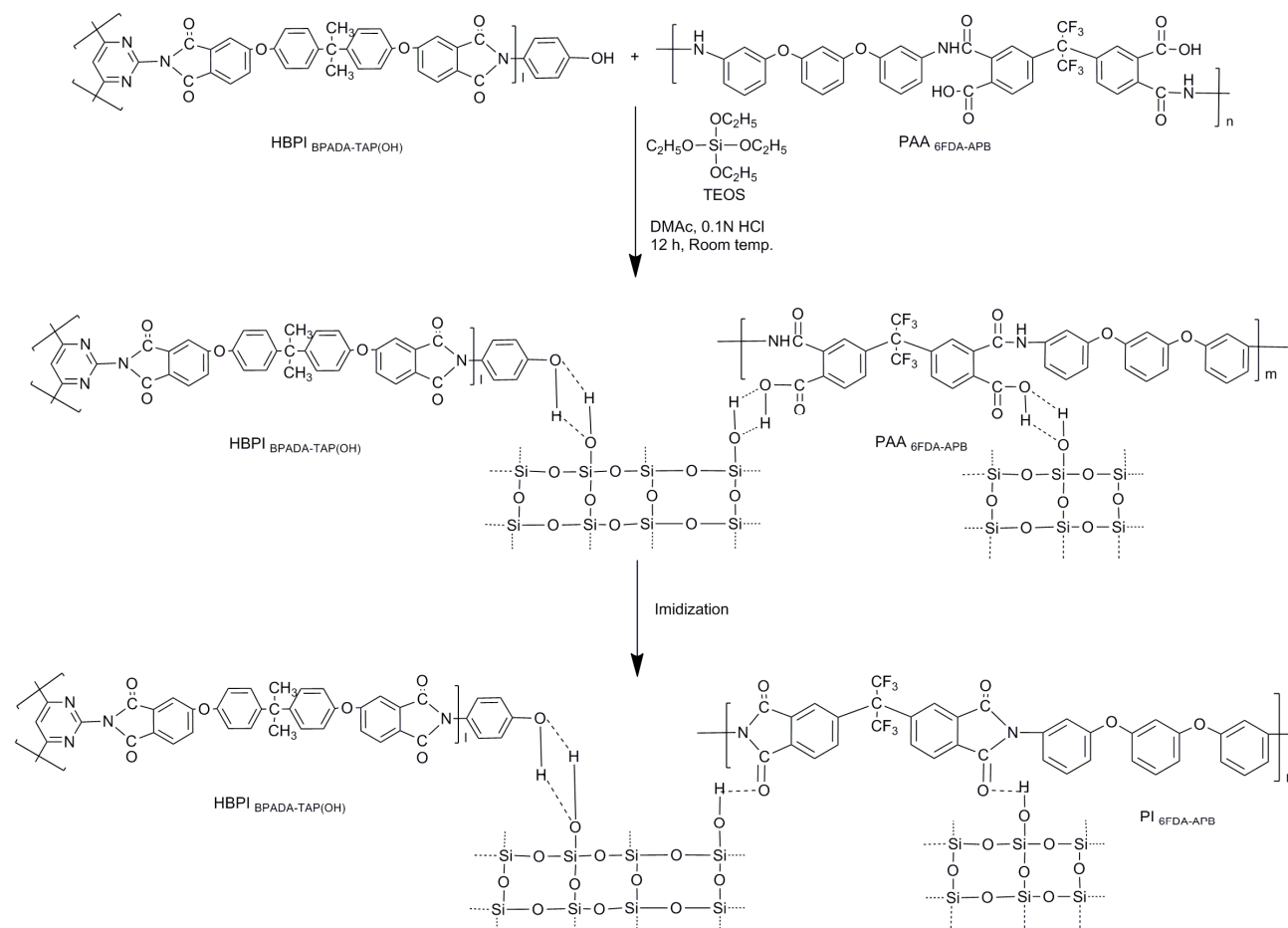
Inorganic Silica linkage Particle

Scheme 1. Illustration of the PI_{6FDA-APB}, HBPI_{BPADA-TAP(OH)}, and SiO₂ linkage network.

Experimental Section

Materials

4,4'-(Hexafluoroisopropylidene)diphthalic anhydride (6FDA, 95%), 2,4,6-triaminopyrimidine (TAP, 98%), 1-hydroxy-cyclohexyl phenyl ketone, and 1,3-bis(3-aminophenoxy)benzene (APB, 98%) were purchased from Adamas-Reagent Co. Ltd. 4,4'-Bis(4'-isopropylidene diphenoxy) bis-(phthalic anhydride) (BPADA, 97%) was purchased from Sigma-Aldrich and Aladdin Chemical Company. 4-Amino-phenol was purchased from Tianjin Chemical Engineering Laboratory. *N,N*-Dimethylacetamide (DMAc, 98%), *N,N*-dimethylmethanamide (DMF, 98%), tetrahydrofuran (THF, 98%), and toluene which were used as the reaction media were purchased from the Beijing Chemical Works and Alfa Aesar. The solvent *N*-methyl-2-pyrrolidone (NMP, 97%) was purchased from Beijing Modern East Fine Chemical. Hydrochloric acid (HCl) and tetraethoxysilane (TEOS, 98%) were purchased from Alfa Aesar and used without further purification. If it is not mentioned specifically, the reactants and solvents were used as received without further purification.



PI_{6FDA-APB}_HBPI_{BPADA-TAP(OH)}_SiO₂ hybrid ternary composite film
 Scheme 2. Synthetic route for the PI_{6FDA-APB}_HBPI_{BPADA-TAP(OH)}_SiO₂ hybrid ternary composites.

5 Synthesis

The synthetic methods for hydroxyl-terminated hyperbranched polyimide and linear polyimide have been described in our previous report.¹³

The synthetic routes of the materials are shown in Schemes 1 and 2, which include the preparations of the hybrid ternary PI_{6FDA-APB}_HBPI_{BPADA-TAP(OH)}_SiO₂ composites. The preparation details are described next.

PI_{6FDA-APB}_HBPI_{BPADA-TAP(OH)}_SiO₂ hybrid ternary composite films. The hybrid ternary composites were prepared by using a typical sol-gel method (Scheme 2). As the composite films were prepared by the similar method, to avoid the redundancy, only the preparation of the composite SC-3 (PI_{6FDA-APB}_HBPI_{BPADA-TAP(OH)}-20%_SiO₂-20%) is given here as a typical example. Stoichiometric quantities of TEOS in DMAc (10 wt%, 1.38 g), and HCl in deionized water (0.1 N, 0.048 g) were mixed and stirred at room temperature for 0.5 h to form the SiO₂ sol. Then, the SiO₂ solution was added dropwise into the solution of

the linear polyamic acid obtained from 6FDA and APB (PAA, 10 wt%, 2 g) and HBPI_{BPADA-TAP(OH)} (0.04 g) with stirring. The mixture was stirred at room temperature for 12 h to obtain the SC-3 (PI_{6FDA-APB}_HBPI_{BPADA-TAP(OH)}-20%_SiO₂-20%) precursor. In the second stage, the precursor solution was cast on a glass plate and heated at 80 °C for 2 h. The film was then thermally imidized by step-wise heating at 150 °C (1 h), 200 °C (1 h), and 300 °C (1 h).

The composite films with different compositions were prepared by a similar method by adjusting the compositions of the PI and silica. The film formation property of the hybrid ternary composite films depended on the contents of the PI_{BPADA-TAP(OH)} and TEOS. And uniform films could be obtained under proper conditions. By using the linear PAA and HBPI, the hybrid ternary composites were prepared successfully. The films are named: SB-1~SB-5 for PI_{6FDA-APB} - HBPI_{BPADA-TAP(OH)}-10% - SiO₂-0% ~ 40% and SC-1~SC-5 for PI_{6FDA-APB} - HBPI_{BPADA-TAP(OH)}-20%-SiO₂-0% ~ 40%, where the percentage given in the generic abbreviations is the weight percentage relative to the

linear PI calculated from the reactant amounts.

FT-IR analysis results

FTIR for SB-1 (KBr, cm^{-1}): 2967 cm^{-1} (CH_3 asym. str.); 1783 cm^{-1} (C=O sym. str.); 1720 cm^{-1} (C=O asym. str.); 1585, 1477 cm^{-1} (C=C str. arom.); 1367 cm^{-1} (C–N str. imide); 1238, 1187 cm^{-1} (Ar–O–Ar), 1137 cm^{-1} ($-\text{CF}_3$); 960, 846 cm^{-1} (Ar–H); 779, 717 cm^{-1} (Subst. Ar.); and 1660–1670 cm^{-1} (Non PAA structure band).

FTIR for SB-2 (KBr, cm^{-1}): 2967 cm^{-1} (CH_3 asym. str.); 1783 cm^{-1} (C=O sym. str.); 1720 cm^{-1} (C=O asym. str.); 1585, 1477 cm^{-1} (C=C str. arom.); 1367 cm^{-1} (C–N str. imide); 1240, 1189 cm^{-1} (Ar–O–Ar), 1137 cm^{-1} ($-\text{CF}_3$); 1068–1003 cm^{-1} (Si–O–Si); 960 cm^{-1} (Ar–H); 890 cm^{-1} (Si–OH); 846 cm^{-1} (Ar–H); 779, 717 cm^{-1} (Subst. Ar.); and 1660–1670 cm^{-1} (Non PAA structure band).

FTIR for SB-3 (KBr, cm^{-1}): 2967 cm^{-1} (CH_3 asym. str.); 1783 cm^{-1} (C=O sym. str.); 1720 cm^{-1} (C=O asym. str.); 1585, 1477 cm^{-1} (C=C str. arom.); 1367 cm^{-1} (C–N str. imide); 1238, 1189 cm^{-1} (Ar–O–Ar), 1137 cm^{-1} ($-\text{CF}_3$); 1071–1003 cm^{-1} (Si–O–Si); 960 cm^{-1} (Ar–H); 890 cm^{-1} (Si–OH); 846 cm^{-1} (Ar–H); 779, 717 cm^{-1} (Subst. Ar.); and 1660–1670 cm^{-1} (Non PAA structure band).

FTIR for SB-4 (KBr, cm^{-1}): 2967 cm^{-1} (CH_3 asym. str.); 1783 cm^{-1} (C=O sym. str.); 1720 cm^{-1} (C=O asym. str.); 1585, 1479 cm^{-1} (C=C str. arom.); 1369 cm^{-1} (C–N str. imide); 1240, 1189 cm^{-1} (Ar–O–Ar), 1137 cm^{-1} ($-\text{CF}_3$); 1068–1003 cm^{-1} (Si–O–Si); 960 cm^{-1} (Ar–H); 890 cm^{-1} (Si–OH); 846 cm^{-1} (Ar–H); 779, 717 cm^{-1} (Subst. Ar.); and 1660–1670 cm^{-1} (Non PAA structure band).

FTIR for SB-5 (KBr, cm^{-1}): 2967 cm^{-1} (CH_3 asym. str.); 1783 cm^{-1} (C=O sym. str.); 1720 cm^{-1} (C=O asym. str.); 1585, 1479 cm^{-1} (C=C str. arom.); 1369 cm^{-1} (C–N str. imide); 1240, 1189 cm^{-1} (Ar–O–Ar), 1137 cm^{-1} ($-\text{CF}_3$); 1060–1003 cm^{-1} (Si–O–Si); 960 cm^{-1} (Ar–H); 890 cm^{-1} (Si–OH); 846 cm^{-1} (Ar–H); 779, 717 cm^{-1} (Subst. Ar.); and 1660–1670 cm^{-1} (Non PAA structure band).

FTIR for SC-1 (KBr, cm^{-1}): 2967 cm^{-1} (CH_3 asym. str.); 1783 cm^{-1} (C=O sym. str.); 1720 cm^{-1} (C=O asym. str.); 1585, 1477 cm^{-1} (C=C str. arom.); 1367 cm^{-1} (C–N str. imide); 1238, 1187 cm^{-1} (Ar–O–Ar), 1137 cm^{-1} ($-\text{CF}_3$); 960, 846 cm^{-1} (Ar–H); 779, 717 cm^{-1} (Subst. Ar.); and 1660–1670 cm^{-1} (Non PAA structure band).

FTIR for SC-2 (KBr, cm^{-1}): 2967 cm^{-1} (CH_3 asym. str.); 1783 cm^{-1} (C=O sym. str.); 1720 cm^{-1} (C=O asym. str.); 1585, 1477 cm^{-1} (C=C str. arom.); 1369 cm^{-1} (C–N str. imide); 1238, 1189 cm^{-1} (Ar–O–Ar), 1137 cm^{-1} ($-\text{CF}_3$); 1070–1003 cm^{-1} (Si–O–Si); 960 cm^{-1} (Ar–H); 890 cm^{-1} (Si–OH); 846 cm^{-1} (Ar–H); 779, 717 cm^{-1} (Subst. Ar.); and 1660–1670 cm^{-1} (Non PAA structure band).

FTIR for SC-3 (KBr, cm^{-1}): 2967 cm^{-1} (CH_3 asym. str.); 1783 cm^{-1} (C=O sym. str.); 1720 cm^{-1} (C=O asym. str.); 1585, 1477 cm^{-1} (C=C str. arom.); 1369 cm^{-1} (C–N str. imide); 1238, 1189 cm^{-1} (Ar–O–Ar), 1137 cm^{-1} ($-\text{CF}_3$); 1068–1003 cm^{-1} (Si–O–Si); 960 cm^{-1} (Ar–H); 890 cm^{-1} (Si–OH); 846 cm^{-1} (Ar–H); 779, 717 cm^{-1} (Subst. Ar.); and 1660–1670 cm^{-1} (Non PAA structure band).

FTIR for SC-4 (KBr, cm^{-1}): 2967 cm^{-1} (CH_3 asym. str.); 1781 cm^{-1} (C=O sym. str.); 1720 cm^{-1} (C=O asym. str.); 1585, 1477 cm^{-1} (C=C str. arom.); 1369 cm^{-1} (C–N str. imide); 1240, 1189 cm^{-1} (Ar–O–Ar), 1137 cm^{-1} ($-\text{CF}_3$); 1068–1003 cm^{-1} (Si–O–Si); 960 cm^{-1} (Ar–H); 890 cm^{-1} (Si–OH); 846 cm^{-1} (Ar–H); 779, 717 cm^{-1} (Subst. Ar.); and 1660–1670 cm^{-1} (Non PAA structure band).

FTIR for SC-5 (KBr, cm^{-1}): 2967 cm^{-1} (CH_3 asym. str.); 1781 cm^{-1} (C=O sym. str.); 1720 cm^{-1} (C=O asym. str.); 1585, 1477

cm^{-1} (C=C str. arom.); 1371 cm^{-1} (C–N str. imide); 1238, 1189 cm^{-1} (Ar–O–Ar), 1137 cm^{-1} ($-\text{CF}_3$); 1064–1003 cm^{-1} (Si–O–Si); 960 cm^{-1} (Ar–H); 890 cm^{-1} (Si–OH); 846 cm^{-1} (Ar–H); 779, 717 cm^{-1} (Subst. Ar.); and 1660–1670 cm^{-1} (Non PAA structure band).

Characterization

Fourier transform infrared (FTIR) spectroscopic measurements were performed using a Magna-IR Nicolet 560 FTIR spectrophotometer by incorporating samples in KBr disks. The spectra were recorded in the range 4000–450 cm^{-1} at a resolution of 0.35 cm^{-1} . The data were calibrated with linear polystyrene standards.

The phase transitions and thermal properties were characterized by differential scanning calorimeter (DSC), thermal gravimetric analysis (TGA) and Dynamic mechanical analysis (DMA). TGA was performed with a TA Instruments TGA 2050 thermo gravimetric analyzer (TA instrument Co.) at a heating rate of 20 $^{\circ}\text{C}$ from room temperature to 900 $^{\circ}\text{C}$ under a continuous flow of nitrogen. Thermal phase transitions of the polymers were scanned by DSC 2910 (TA Instrument Co.) with a heating rate of 20 $^{\circ}\text{C min}^{-1}$ under nitrogen atmosphere flow. The dielectric constants were determined using a NOVOCOOL Alpha-ANB (Novocontrol Technologies GmbH & Co. KG) dielectric analyzer with silver paint electrode, at the room temperature with scan frequencies from 10^6 Hz to 1 Hz, and the reference was a commercial Kapton® HN type PI ($D_k = 3.81$ at 100 kHz). The thickness of specimens was controlled to be 14–41 μm . The coefficient of thermal expansion (CTE) parallel to the film surfaces were measured using a DMA Q800 dynamic mechanical analyzer (TA Instrument Co.) in extension mode over a temperature range from 25 to 320 $^{\circ}\text{C}$ with a force of 0.01 N. The samples used for the measurements were 14 mm in length, 5 mm in width, and 21–55 μm in thickness.

UV-visible absorption spectra of films were measured on a Lambda Bio-40 spectrometer (Perkin-Elmer). Cross-sectional images of the polyimide hybrid films were studied by scanning electron microscopy (SEM). The SEM images were obtained using a S5500 microscope (Hitachi) operating at an acceleration voltage of 5.0 kV.

Results and Discussion

Synthesis and Characterization

By using PAA of the linear PI ($\text{PI}_{6\text{FDA-APB}}$), hyperbranched polyimide ($\text{HBPI}_{\text{BPADA-TAP(OH)}}$) and TEOS, the hybrid ternary composites with different compositions were prepared by the sol-gel method. In the following discussion, the composites are referred to as the SB series ($\text{PI}_{6\text{FDA-APB}}\text{-HBPI}_{\text{BPADA-TAP(OH)}}\text{-10\% SiO}_2\text{-0\%~40\%}$, SB-1~SB-5) and the SC series ($\text{PI}_{6\text{FDA-APB}}\text{-HBPI}_{\text{BPADA-TAP(OH)}}\text{-20\% SiO}_2\text{-0\%~40\%}$, SC-1~SC-5). The percentages given in the genetic abbreviations are the weight percentage. As discussed below, the physical properties with different contents of SiO_2 can be compared when the concentrations of the hyperbranched polyimide are fixed at two representative values 10% and 20%, respectively.

The FTIR spectra of the hybrid ternary composites and $\text{HBPI}_{\text{BPADA-TAP(OH)}}$ are shown in Fig. 1 (Fig. 1(a) and 1(b) for SB

and SC series). In the FTIR spectra, the absorption bands of imide structure are clearly observed at 1785-1781 and 1731-1720 cm^{-1} for the symmetric and anti-symmetric stretching vibrations of the carbonyl groups. There are no obvious absorption bands of polyamic acid (PAA) between 1660 and 1670 cm^{-1} , which proves that the PI precursors were fully imidized.

The FTIR spectra of hybrid ternary composite films show some characteristics related to the SiO_2 network formation. The sol-gel process containing TEOS can be viewed as a network forming process. A very weak absorption appeared at 890 cm^{-1} and strong absorption at 1071-1003 cm^{-1} for the hybrid ternary composite films (SB-2~SB-5 and SC-2~SC-5) are attributed to the presence of a tiny amount of Si-OH groups and dominant Si-O-Si networks formed during the hydrolysis of alkoxy groups in TEOS. Above results verify the not only PAA is completely converted to PI and but also the SiO_2 networks are formed in the organic-inorganic composite through the sol-gel process.

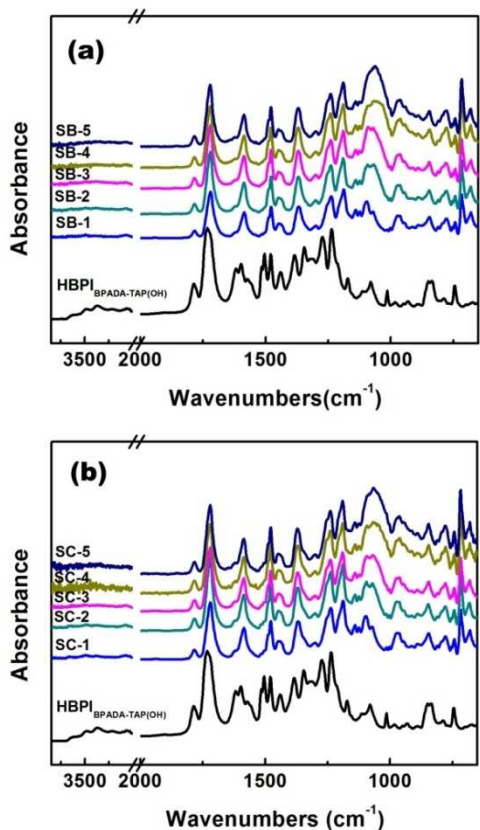


Fig. 1 FTIR spectra of $\text{HBPI}_{\text{BPADA-TAP(OH)}}$ and hybrid ternary composites, (a) SB series, (b) SC series.

Although the spectral characteristics are similar for the composites, there are some differences for their FTIR spectra. For both SB-2~SB-5 and SC-2~SC-5, the spectra show a gradual increase in absorbance at the bands around 1071-1003 cm^{-1} (Si-O-Si symmetric stretching vibrations) with the increase of TEOS concentration in the precursors. Although there are a large amount of hydroxyl groups in $\text{HBPI}_{\text{BPADA-TAP(OH)}}$ and silica network of TEOS, the absorption bands related with the hydroxyl groups can no longer be seen in the spectra after the sol-gel

transformation. It means that the hydroxyl groups in $\text{HBPI}_{\text{BPADA-TAP(OH)}}$ participate in the inorganic silica network formation process. The organic-inorganic interactions become stronger with increasing of $\text{HBPI}_{\text{BPADA-TAP(OH)}}$ concentration in the process.

Dielectric properties

Fig. 2 shows that the dielectric constants (D_k) of the composite films and related materials measured in the frequency range from 10^6 Hz to 1 Hz and measured at a fixed frequency (100 kHz). The dielectric constants show an increase with decreasing frequency, which is a typical frequency dependence behavior of dielectric properties,²⁷ that can be described by Cole-Cole equation model.²⁸

$$\varepsilon^* - \varepsilon_\infty = (\varepsilon_0 - \varepsilon_\infty) / [1 + (i\omega\tau_0)^{1-\alpha}] \quad (1)$$

In above equation (1), ε^* is the complex dielectric constant, ε_0 and ε_∞ are the dielectric constants at “static” and “infinite frequency”, $\omega = 2\pi$ times the frequency, and τ_0 is a generalized relaxation time. The exponent parameter α can assume a certain value between 0 and 1, in which the former case corresponds to the result by Debye for polar dielectrics.²⁸

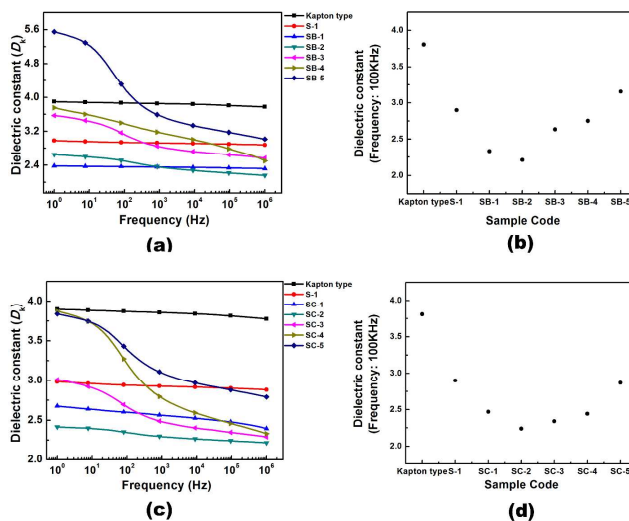


Fig. 2 Dielectric constant (D_k) of the hybrid ternary composite films and related materials, (a) the SB series with scanning frequency from 10^6 to 1, (b) the SB series measured at frequency = 100 kHz SC, (c) the SB series with scanning frequency from 10^6 to 1, (d) the SB series measured at frequency = 100 kHz.

Compared with the two PIs, the Kapton® HN type PI and $\text{PI}_{\text{6FDA-APB}}$ (S-1), the dielectric constants of the organic-inorganic composites show a more significant dependence on the frequency (Fig. 2(a) and 2(c)). Especially, for SB-4, SB-5 and SC-5, which have the high concentrations of SiO_2 , significant dielectric dispersion can be seen in the range from 10^3 to 1 Hz. It is caused by the increased space charge polarization between organic and inorganic phase. As it will be discussed below, the strong phase separation between the inorganic silica networks and PIs will occur in case for the higher concentrations of SiO_2 without sufficient $\text{HBPI}_{\text{BPADA-TAP(OH)}}$ to stabilize the inorganic phase. In the high frequency range ($> 10^3$ Hz), the dielectric constants of the composites, except those with strong phase separation (SB-4,

SB-5 and SC-5), are obviously lower than $PI_{6FDA-APB}$ (S-1). It is interesting to observe that $HBPI_{BPADA-TAP(OH)}$ shows a significant effect to reduce the dielectric constant, which can be seen by comparing the D_k values of SB-1 and SC-1 with that of S-1. For the hybrid ternary composites with a proper amount of SiO_2 , the dielectric constants can be further reduced as shown by comparing the D_k values for SC-1 and SC-2.

This tendency can be more clearly seen from Fig. 2(b) and 2(d) that give the dielectric constants of all the films measured at 100 kHz with the sample code as the ordinates. The dielectric constant determined at 100 kHz is usually used to identify the ability of the polarizable units to orient fast enough to keep up with the applied current electric insulator device fields. When the content of $HBPI_{BPADA-TAP(OH)}$ is fixed at 10 wt% and 20 wt% (for SB and SC series), even without the addition of SiO_2 , $HBPI_{BPADA-TAP(OH)}$ shows significant effect to reduce the dielectric constants. After adding 10% SiO_2 into the system, the dielectric constants of both series can further decrease. SB-2 ($PI_{6FDA-APB-HBPI(OH)-10\%SiO_2-10\%}$) shows the smallest dielectric constant ($D_k = 2.26$) in the SB series. For the SC series, the lowest value ($D_k =$

2.36) is obtained for SC-3 ($PI_{6FDA-APB-HBPI(OH)-20\%SiO_2-20\%}$). However, when the amounts of SiO_2 further increase, dielectric constants gradually increase (SB-3~SB-5 and SC-4, SC-5) due to the aggregation and inhomogeneous dispersion of silica network.

The effect of $HBPI_{BPADA-TAP(OH)}$ to reduce the dielectric constants can be attributed to nano-scale cavities (typically several angstroms in size) in the branched structure for hyperbranched polymers.^{6, 21, 22} Moreover, the HBPI component can also enhance the homogeneous dispersion of silica in the system, as it will be shown by the morphology observation and the UV-Vis spectroscopy discussed below. Because $HBPI_{BPADA-TAP(OH)}$ can improve the inorganic-organic phase dispersion, it plays a very important role not only in reducing the dielectric constant of hybrid ternary composite films, but also in reduced space charge polarization at the same time. This point can be clearly seen from the curves for SB-2 and SC-2 in Fig. 2(a) and 2(c), which show less significant reliance on the frequency. The SEM observation confirms $HBPI_{BPADA-TAP(OH)}$ can counter-balance the tendency towards phase separation when SiO_2 concentration is not too high.

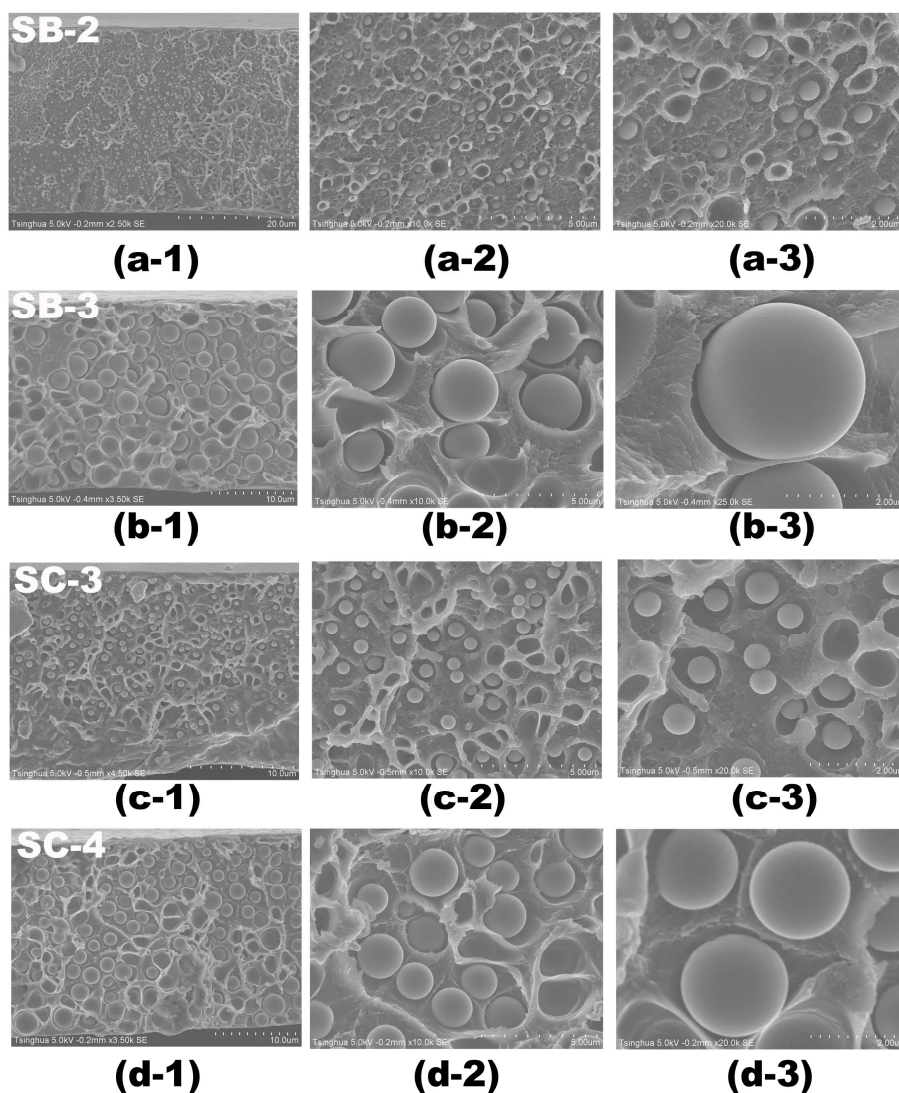


Fig. 3 Typical SEM images of the hyperbranched polyimide with PI/SiO_2 hybrid ternary composite films, (a) SB-2, (b) SB-3, (c) SC-3, (d) SC-4; Scale bar: 20 μm (a-1), 10 μm (b-1, c-1, d-1), 5 μm (a-2), 2 μm (a-3, b-3, c-3, d-3).

Table 1 The parameters and properties of hydroxyl terminated hyperbranched polyimide with PI/SiO₂ hybrid ternary composites.

Sample	Thickness ^a μm	D_k ^b	λ_{cutoff} nm	Transmittance		DSC	TGA		R_{w800} ^d %	CTE ^c ppm °C ⁻¹
				450 nm/ %	400 nm/ %	T_g / °C	$T_d^{5\% c}$ / °C	$T_d^{10\% c}$ / °C		
SB-1 PI_HBPI(OH)-10%	27	2.36	316	92	77	205.0	538	561	57	38.3
SB-2 PI_HBPI(OH)-10%_SiO ₂ -10%	14	2.26	327	16	6	196.3	527	557	53	26.6
SB-3 PI_HBPI(OH)-10%_SiO ₂ -20%	24	2.67	327	2	1	197.6	487	552	58	20.9
SB-4 PI_HBPI(OH)-10%_SiO ₂ -30%	39	2.75	326	1	1	199.8	478	553	53	15.9
SB-5 PI_HBPI(OH)-10%_SiO ₂ -40%	18	3.22	328	1	1	201.6	352	538	62	17.7
SC-1 PI_HBPI(OH)-20%	40	2.65	325	86	65	202.8	517	552	57	32.9
SC-2 PI_HBPI(OH)-20%_SiO ₂ -10%	41	2.62	327	63	41	200.7	517	553	55	28.1
SC-3 PI_HBPI(OH)-20%_SiO ₂ -20%	27	2.36	324	9	4	200.5	487	547	57	23.1
SC-4 PI_HBPI(OH)-20%_SiO ₂ -30%	20	2.40	327	8	7	200.8	424	536	60	17.6
SC-5 PI_HBPI(OH)-20%_SiO ₂ -40%	36	3.50	326	1	0.5	200.1	379	531	62	20.8

^a The thickness of specimens for dielectric constant measurement.

^b Measuring at frequency of 100 kHz.

^c Temperatures at which 5% and 10% weight loss occurred, respectively, recorded by TGA at a heating rate of 20 °C/min and a N₂ gas flow rate of 25 cm³ min⁻¹.

^d Residual weight percentages at 800 °C.

^e The temperature range from 100 to 150 °C with a force of 0.01 N.

Morphology

Fig. 3 shows the typical SEM images of the selected composites films. The silica loading and reinforcement binding with PI₆FDA-APB_HBPI_{BPADA-TAP(OH)} matrix can be confirmed by the morphology. Fig. 3(a) and 3(c) show improved phase dispersion morphology between HBPI_{BPADA-TAP(OH)} and SiO₂. It can be seen that the hybrid ternary system displays good phase dispersion between organic PIs and inorganic silica. When the SiO₂ concentration is not too high, HBPI_{BPADA-TAP(OH)} can prevent the observable phase separation of silica and lead to a homogenous distribution of SiO₂ networks. However, when the amount of SiO₂ is large, such as SB-3 and SC-4 (Fig. 3(b) and 3(d)), the SEM images evidence the unbounded silica particles and the interfacial voids by the weak interaction between the organic phase and silica inorganic phase. The aggregated silica phase can be seen as spherical particles with an average diameter increasing from 300 nm in SB-2 to 3 μm in SB-3 and from 400 nm in SC-3 to 2 μm in SC-4 with the increase of the amount of SiO₂, respectively.

Optical properties

The optical transparency of all the hybrid ternary composites (SB and SC series) and PI₆FDA-APB films (S-1), was measured with UV-Vis spectroscopy. Fig. 4 shows the UV-Vis transmission spectra. The cutoff wavelengths (absorption edge, λ_{cutoff}) and transmittance at 450 nm and 400 nm obtained from these spectra are listed in Table 1.

By comparing the UV-Vis spectra of the PIs (S-1, SB-1, SC-1) with composites, i.e., SB Series (PI₆FDA-APB_HBPI_{BPADA-TAP(OH)}-10%_SiO₂-0%~40%) and SC series (PI₆FDA-APB_HBPI_{BPADA-TAP(OH)}-20%_SiO₂-0%~40%), it can be seen that the transparency of the films decreases with the increase of the SiO₂ content. The inorganic silica phase in the system causes light scattering at widely wavelength region with the increase of the inorganic silica content and results in the opacity of the films. This is consistent with the morphology observed by SEM. On the other hand, when the content of HBPI_{BPADA-TAP(OH)} increases from 10 to 20 %, the transparency of films was significantly improved at the same

SiO₂ content. This effect is obvious when comparing the transmittance of SB-2 and SC-2 as well as the other samples in the SB and SC series.

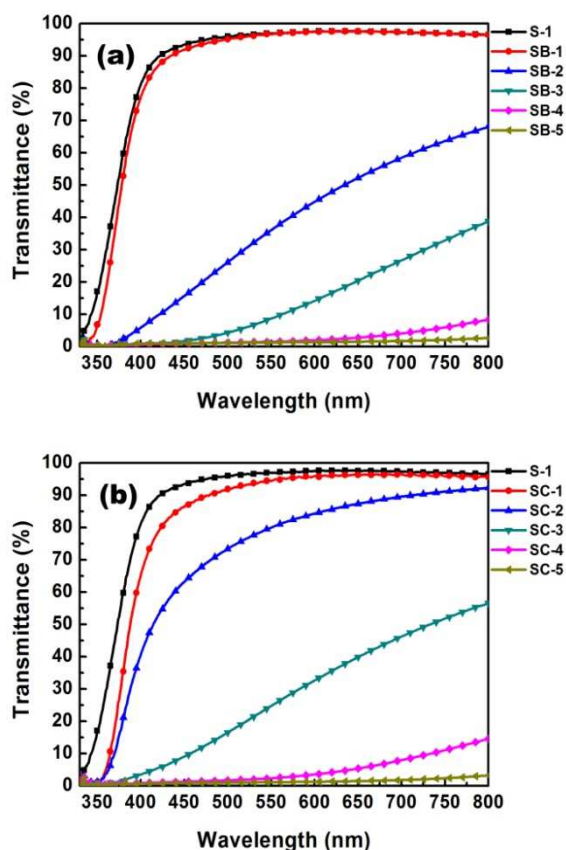


Fig. 4 UV-Vis spectra of the hybrid ternary composite films and PIs from 800 to 320 nm wavelength, (a) SB series (PI₆FDA-APB_HBPI_{BPADA-TAP(OH)}-10%_SiO₂-0%~40%) and (b) SC series (PI₆FDA-APB_HBPI_{BPADA-TAP(OH)}-20%_SiO₂-0%~40%) group.

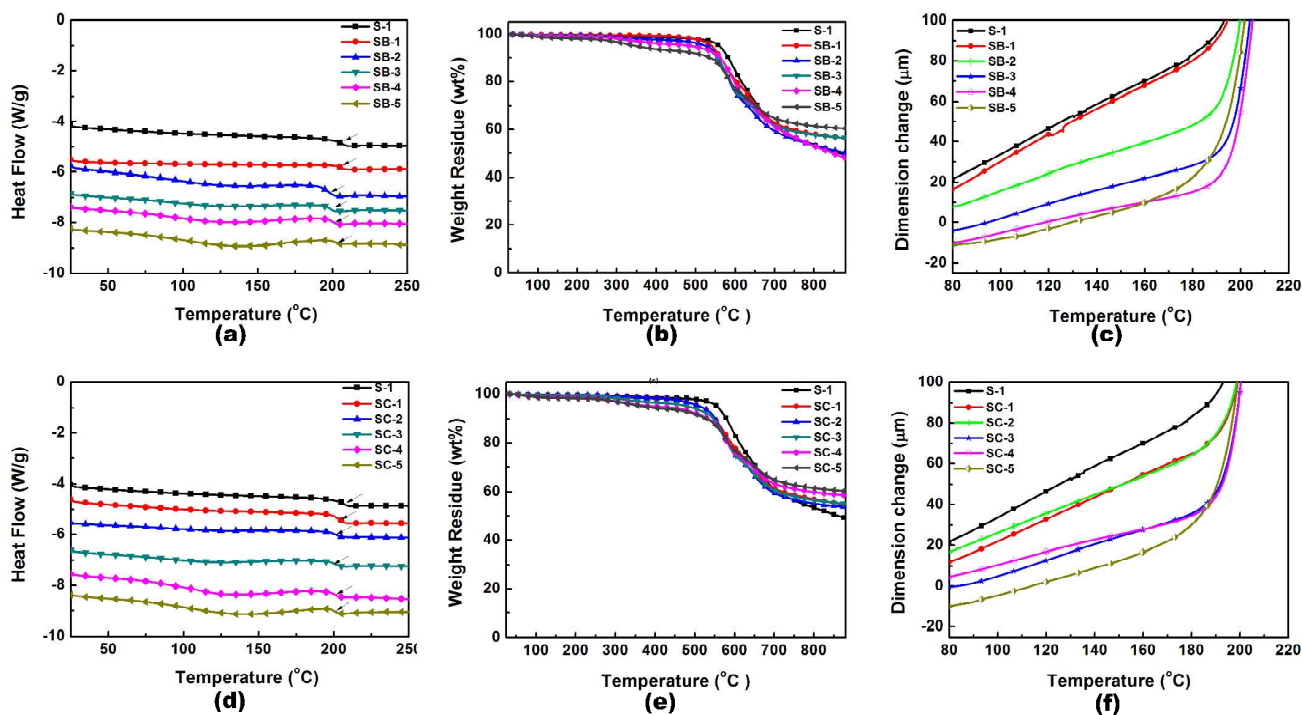


Fig. 5 DSC (a, d), TGA (b, e) and CTE (c, f) curves of the hybrid ternary composite films and PIs, (a), (b), (c) SB series ($\text{PI}_{6\text{FDA-APB}}\text{-HBPI}_{\text{BPADA-TAP(OH)}}\text{-10\%}_\text{SiO}_2\text{-0\%}\sim\text{40\%}$) and (d), (e), (f) Series SC ($\text{PI}_{6\text{FDA-APB}}\text{-HBPI}_{\text{BPADA-TAP(OH)}}\text{-20\%}_\text{SiO}_2\text{-0\%}\sim\text{40\%}$).

5

All the results of dielectric measurements, morphology observation, and UV-Vis spectroscopy indicate that the $\text{HBPI}_{\text{BPADA-TAP(OH)}}$ has an apparent effect to reduce the phase separation between organic PIs and inorganic silica. This effect can be attributed to the hydroxyl groups of $\text{HBPI}_{\text{BPADA-TAP(OH)}}$, which introduce the linkage with the silica network and reduce the phase separation between PI and silica network. $\text{HBPI}_{\text{BPADA-TAP(OH)}}$ is compatible with $\text{PI}_{6\text{FDA-APB}}$ through intermolecular hydrogen bonding and other intermolecular interactions. It can be linked to the inorganic silica networks during transformation of TEOS from Si-OH to SiO_2 . This enhanced interaction among the components can effectively reduce the light scattering by minimizing the size of silica phase.

Thermal properties

The thermal phase transition behavior of the hybrid ternary composites and PIs was investigated by DSC as shown in Fig. 5(a), (d), and those summarized at Table 1. It can be seen that only single glass transition temperature T_g is observed for all the films. The SB and SC series show T_g values in the ranges 205.0 to 196.3 °C and 202.8 to 200.1 °C, respectively. After incorporating $\text{HBPI}_{\text{BPADA-TAP(OH)}}$ or/and SiO_2 in the composites, the T_g s of materials vary in few degree scale compared with that of the linear PI (S-1). It indicates that the addition of $\text{HBPI}_{\text{BPADA-TAP(OH)}}$ and SiO_2 components does not show obvious effects on the glass transition temperature.

The thermal decomposition of the hybrid composites and PIs was monitored by the TGA analysis. The results are shown in Fig. 5 (b), (e) and also summarized in Table 1. The residual weights of

series SB and SC are nearly 100 % for all the samples below 300 °C. The 5% and 10% weight losses for $\text{PI}_{6\text{FDA-APB}}$ are 549 and 571 °C, respectively. When 10% and 20% of $\text{HBPI}_{\text{BPADA-TAP(OH)}}$ exist, the 5% weight loss decreases to 538 and 517 °C for SB-1 and SC-1, and the 10% weight loss decreases to 561 and 552 °C, respectively. It means the thermal stability decreases when adding the hyperbranched PI into the systems. For the hybrid ternary composites, the thermal stability decreases with the increase of the inorganic component. When the $\text{HBPI}_{\text{BPADA-TAP(OH)}}$ content is 10%, the 5% and 10% weight losses are 527 and 557 °C for 10% of SiO_2 (SB-2). When the $\text{HBPI}_{\text{BPADA-TAP(OH)}}$ content is 20%, the 5% and 10% weight losses are 517 and 553 °C for 10% of SiO_2 (SC-2). When the SiO_2 content further increases, the thermal stability shows a more obvious decrease. Especially, when the SiO_2 content is 40%, the 5% weight loss of the composites decreases to 352 and 379 °C for SB-5 and SC-5, and the 10% weight loss decreases to 538 °C and 531 °C, respectively. These observations are attributable to the incomplete hydrolysis reaction of TEOS during the sol-gel process when the concentration is too high.

The thermal expansion curves are shown in Figs. 5(c), (f), and the CTE values are listed in Table 1. The dramatic increase at higher than 200 °C is related to the glass transitions as revealed by the DSC analysis. Typical CTE values for conventional PIs are 30 to 60 $\text{ppm } ^\circ\text{C}^{-1}$ ²⁹⁻³², and our previous study has shown that the CTE for $\text{PI}_{6\text{FDA-APB}}$ (S-1) is 37.1 $\text{ppm } ^\circ\text{C}^{-1}$ in the range of 100–150 °C.¹³ According to previous articles and our study,^{13, 29-33} the small CTE values are mainly attributed to the polymer structure and composite compositions. If it has a relatively rigid

or planar structure in the backbone like Kapton® HN type PI (CTE = 32 ppm °C⁻¹ in the range of 100-200 °C), the CTE can be lowered. However, such structures often cause intra- and intermolecular charge-transfer (CT) interactions leading to yellowish color.³³ On the contrary, the bulky side groups and kinked structures in the backbone of PI_{6FDA-APB} (S-1) effectively suppress preferential in-plane orientation and stretching of the main chains, which slightly increases the CTE, but affords transparent and colorless films owing to the suppressed CT-interactions.³³ The CTEs of SB-1 and SC-1 are larger than that of linear PI (S-1), and the CTE of SB-1 is larger than SC-1 with increasing the amount of HBPI_(OH). This is attributed to the facts that HBPI_(OH) includes not only bulky -CH₃ groups but also many hydroxyl terminated groups which can form hydrogen bondings with linear PI backbone matrices.²⁹

With incorporation of inorganic silica components, CTE of the hybrid ternary composites is effectively reduced due to three-dimensional cross-linking structures and intrinsically small CTE of silica. Even with 10% of SiO₂, the CTEs of SB-2 and SC-2 were reduced to 26.1 and 28.1 ppm °C⁻¹, respectively. There exists covalent bondings and intense molecular interactions by hydrolysis reaction with containing silica materials between linear PI backbone and HBPI_(OH) of which partial hydrogen bonding of HBPI_(OH) with linear PI backbone is dispersed into the silica networks. The CTE of the SB-4 (PI_{6FDA-APB}-HBPI_{BPADA-TAP(OH)}-10%_SiO₂-30%) is the smallest in the series, which is 15.9 ppm °C⁻¹ compared to 37.1 ppm °C⁻¹ of PI with the decrease by 59%. The SC-4 (PI_{6FDA-APB}-HBPI_{BPADA-TAP(OH)}-20%_SiO₂-30%) also shows a significant reduction from 37.1 ppm °C⁻¹ for the linear PI to 17.6 ppm °C⁻¹, which is reduced by 52%. As a result of the formed silica network, the CTE values reduce with the increasing amount of inorganic silica in the composites. The CTEs of SB-5 and SC-5 are larger than those of the other hybrid ternary composites, which is attributable to the macro-phase separation with too high SiO₂ concentrations. The residual stress induced by CTE mismatch between PI and glass substrate could sometimes affect the CTEs of the resultant films even after peeling from the substrates.³⁴ The CTEs of PI/silica hybrids might be affected by glass substrate having small CTE. However, we believe that the effect should be minor compared with the factors discussed above.

Based on the above result, a 30% amount of SiO₂ is required to reach the lowest value of CTE (SB-4 and SC-4). On the other hand, a lower SiO₂ content is suitable to achieve the optimized dielectric property and optical transparency. It can be seen that inorganic silica can be complementary at CTE drawbacks of the binary system (SB-1 and SC-1). Even a 10% amount of SiO₂ can reduce the CTE value significantly. On the other hand, HBPI_{BPADA-TAP(OH)} has an effect to reduce D_k and prevent the organic-inorganic phase separation in a certain range. Therefore, the properties of the hybrid ternary composites can be optimized dependent on the potential applications.

Conclusion

The properties of two series of the hybrid ternary composites composed of PI_{6FDA-APB}, HBPI_{BPADA-TAP(OH)}, and various amounts of SiO₂ are systematically investigated. In a proper composition

of HBPI_{BPADA-TAP(OH)} and SiO₂, the lowest dielectric constant (D_k) was achieved for the hybrid ternary composite. The D_k of SB-2 (PI_{6FDA-APB}-HBPI_{BPADA-TAP(OH)}-10%_SiO₂-10%) reaches the lowest value of 2.26 in the series. The effect of HBPI_{BPADA-TAP(OH)} to reduce the D_k values can be attributed to nano-scale cavities in the branched structure for the hyperbranched polymers as well as its ability to prevent the organic and inorganic phase separation. The optical transmittance of the hybrid ternary composite films is significantly improved by incorporation of HBPI_{BPADA-TAP(OH)}. It is caused by the effect of HBPI_{BPADA-TAP(OH)} to reduce the size of silica particles through enhanced interactions among the components. The best result in the hybrid ternary composite films is obtained for SC-2 (PI_{6FDA-APB}-HBPI_{BPADA-TAP(OH)}-20%_SiO₂-10%), which shows the transmittance 63% at 450 nm. By adding silica component, the CTE of the hybrid ternary composites are significantly smaller than that of linear PI (PI_{6FDA-APB}). SB-4 (PI_{6FDA-APB}-HBPI_{BPADA-TAP(OH)}-10%_SiO₂-30%) shows the smallest CTE of 15.9 ppm °C⁻¹ in the series. By comparing to the CTE of 37.1 ppm °C⁻¹ for PI_{6FDA-APB}, it is reduced by 59%. The hybrid ternary composite films fabricated with HBPI_{BPADA-TAP(OH)} or/and inorganic silica are promising materials with the improved characteristics of dielectric, optical and thermal resistant properties, which is quite satisfied to meet the requirements for interlayer dielectrics in advanced electronic devices.

Acknowledgement

The financial support from National Basic Research Program of China (973 Program) under Project 2011CB606102 and that for the stay of X. W. in Tokyo from Tokyo Institute of technology are gratefully acknowledged.

Reference

- S. H. Choi and S. J. Song, *Polym. Sci. & Tech.*, 2005, **16**, 20.
- H. Chen, L. Xie, H. Lu and Y. Yang, *J. Mater. Chem.*, 2007, **17**, 1258.
- L. Tan, S. M. Liu, F. Zeng, Z. Y. Lin and J. Q. Zhao, *Polym. Adv. Technol.*, 2010, **21**, 435.
- Y. H. Zhang, Z. M. Dang, J. H. Xin, W. A. Daoud, J. H. Ji, Y. Y. Liu, B. Fei, Y. Q. Li, J. T. Wu, S. Y. Yang and L. F. Li, *Macromol. Rapid Commun.*, 2005, **26**, 1473.
- Y. H. Zhang, S. G. Lu, Y. Q. Li, Z. M. Dang, H. H. Xin, S. Y. Fu, G. T. Li, R. R. Guo and L. F. Li, *Adv. Mater.*, 2005, **17**, 1056.
- J. C. Huang, P. C. Lim, L. Shen, P. K. Pallathadka, K. Y. Zeng and C. B. He, *Acta Mater.*, 2005, **53**, 2395.
- V. E. Yudin, J. U. Otaigbe, S. Gladchenko, B. G. Olson, S. Nazarenko, E. N. Korytkova and V. V. Gusarow, *Polymer*, 2007, **48**, 1306.
- G. F. Zhao, T. Ishizaka, H. Kasai, M. Hasegawa, T. Furukawa, H. Nakanishi and H. Oikawa, *Chem. Mater.*, 2009, **21**, 419.
- E. Hamciuc, C. Hamciuc and M. Olariu, *Polym. Engin. & Sci.*, 2009, **50**, 520.
- Y. T. Chern and J. Y. Tsai, *Macromolecules*, 2008, **41**, 9556.
- H. Deligöz, S. Özgümüş, T. Yalçınıyuva, S. Yildirim, D. Değer and K. Ulutaş, *Polymer*, 2005, **46**, 3720.
- H. W. Wang, R. X. Dong, H. C. Chu, C. K. Chang and W. C. Lee, *Mater. Chem. & Phys.*, 2005, **94**, 42.
- S. K. Kim, X. Y. Wang, S. J. Ando and X. G. Wang, *RSC Adv.*, 2014, **4**, 27267.
- Y. H. Kim and O. W. Webster, *J.A.M. Chem. Soc.*, 1990, **112**, 4592.
- D. J. Massa, K. A. Shriner, S. R. Turner and B. I. Voit, *Macromolecules*, 1995, **28**, 3214.
- P. J. Flory, *J.A.M. Chem. Soc.*, 1952, **74**, 2718.
- H. R. Kricheldorf, Q. Z. Zang and G. Schwarz, *Polymer*, 1982, **23**, 1821.

-
18. T. Suzuki and Y. Yamada, *J. Polym. Sci. part B: Polym. Phys.*, 2006, **44**, 291.
19. K. L. Wang, M. Jikei and M. A. Kakimoto, *J. Polym. Sci. part A. Polym. Chem.*, 2004, **42**, 3200.
- 5 20. T. Suzuki, Y. Yamada and Y. Tsujita, *Polymer*, 2004, **45**, 7167.
21. Y. J. Lee, J. M. Huang, S. W. Kuo and F. C. Chang, *Polymer*, 2005, **46**, 10056.
22. T. Seçkin, S. Köytepe and H. İ. Adıgüzel, *Mater. Chem. & Phys.*, 2008, **112**, 1040.
- 10 23. S. Baskaran, J. Liu, K. Domansky, N. Kohler, X. Li, C. Coyle, G. E. Fryxell, S. Thevuthasan and R. E. Willford, *Adv. Mater.*, 2000, **12**, 291.
24. Y. J. Lee, J. M. Huang, S. W. Kuo, J. S. Lu and F. C. Chang, *Polymer*, 2005, **46**, 173.
- 15 25. J. Hao, M. Jikei and M. Kakimoto, *Macromolecules*, 2002, **35**, 5372.
26. F. Jianhua, K. Hidetoshi and O. Kenichi, *Macromolecules*, 2000, **33**, 4639.
27. J. O. Simpson and A. K. St.Clair, *Thin Solid Films*, 1997, **308-309**, 480.
- 20 28. K. S. Cole and R. H. Cole, *J. Chem. Phys.*, 1941, **9**, 341.
29. A. Al Arbash, Z. Ahmad, F. Al-Sagheer and A.A.M. Ali, *J. Nanomater.*, 2006, **58648**, 1.
30. J. K. Lee and S. H. Kim, *Fib. Technol. & Indus.*, 2007, **11**, 251.
31. S. X. Lu, P. Cebe and M. Capel, *Polymer*, 1996, **37**, 2999.
- 25 32. R. E. Southward, D. S. Thompson, T. A. Thornton, D. W. Thompson and A.K. St Clair, *Chem. Mater.*, 1998, **10**, 486.
33. Y. S. Jung, Y. S. Yang, S. M. Kim, H. S. Kim, T. G. Park and B. W. Yoo, *Eur. Polym. J.*, 2013, **49**, 3642.
34. H. S. Chung, C. K. Lee, Y. I. Joe and H. S. Han, *Journal of the Korean Institute of Chemical Engineers*, 1998, **36**, 329.
- 30

Hybrid Ternary Composites of Hyperbranched and Linear Polyimides with SiO₂: A Research for Low Dielectric Constant and Optimized Properties

Seongku Kim,^a Xingyuan Wang,^a Shinji Ando,^b
Xiaogong Wang^{a,*}

Graphical Abstract

The hybrid ternary composites with low dielectric constant and high thermal stability were fabricated through composition optimization by introducing suitable amounts of inorganic silica and hyperbranched polyimide into a linear polyimide system.

